# Mössbauer study on $CsFeCl_3$ and $RbFeCl_3$

P. A. Montano
*Department of Physics, University of California, Santa Barbara, California 93106*

Hanan Shechter and E. Cohen
*Department of Physics, Technion-Israel Institute of Technology, Haifa, Israel*

J. Makovsky
*Nuclear Research Center-Negev, Beer Sheva, Israel*

(Received 14 May 1973)

The Mössbauer spectra of $CsFeCl_3$ and $RbFeCl_3$ single crystals have been studied in the temperature range 4.2–300 °K. The temperature dependence of the quadrupole splitting (QS), center shift (CS), and $f$ factor were obtained. It is shown that the single-ion parameters for the $^5T_{2g}$ level of $Fe^{2+}$ are similar in both crystals: $\lambda = 78 \pm 5$ cm$^{-1}$, $\Delta/\lambda = -0.88$ and $-0.78$ for $CsFeCl_3$ and $RbFeCl_3$, respectively. Mössbauer measurements of $CsFeCl_3$ down to 1.4 °K show no transition to three-dimensional ordered state. ($RbFeCl_3$ orders at 2.45 °K.) When the magnetic interaction between the lowest $s = 1$ crystal field state of $Fe^{2+}$ is taken into consideration, the following parameters fit best the QS spectra: $D = 13 \pm 1$ and $12 \pm 1$ cm$^{-1}$, $J_{\parallel} = 2.5 \pm 0.5$ and $5 \pm 1$ cm$^{-1}$, $J_{\perp} = 5 \pm 1$ and $11 \pm 2$ cm$^{-1}$ for $CsFeCl_3$ and $RbFeCl_3$, respectively. From the temperature dependence of the CS and $f$ factor, effective Einstein and Debye temperatures are deduced: $\Theta_E = (204 \pm 22)$ °K, $\Theta_D = (185 \pm 25)$ °K for $CsFeCl_3$; and $\Theta_E = (310 \pm 45)$ °K, $\Theta_D = (260 \pm 30)$ °K for $RbFeCl_3$.

## I. INTRODUCTION

In this work we report the results of a comparative study of Mössbauer results of $RbFeCl_3$ and $CsFeCl_3$. In a recent report[1] the analysis of the behavior of the electric field gradient (EFG) and the susceptibility in $RbFeCl_3$ were discussed in detail: It was shown that at low temperatures the iron-iron interaction along the hexagonal $c$ axis is ferromagnetic, where a magnetic iron-pair interaction was assumed. In the low-temperature region (below 70 °K) the $RbFeCl_3$ system could be described by an effective spin Hamiltonian with $s = 1$. Since $CsFeCl_3$ is isomorphous with $RbFeCl_3$ it is interesting to try a comparative study of these two nearly-one-dimensional systems. The quadrupole shift (QS), the center shift (CS), and the Mössbauer spectral area were measured as a function of temperature, and the results are discussed.

## II. EXPERIMENT

The samples were cut from grown single crystals of $RbFeCl_3$ and $CsFeCl_3$. A commercial helium cryostat (Ricor, MCH-5B) was used for sample ambient temperature. A Janis cryostat was also used to reduce the temperature to 1.4 °K. The temperature above 4.2 °K was regulated by controlling the helium flow through the Ricor cryostat. Below 10 °K the stability was kept within ± 0.5 °K. The source used was 25-mC; $^{57}$Co in palladium matrix. The spectra were recorded on an on-line computerized spectrometer operating in a constant-acceleration mode, and the spectra were analyzed by a nonlinear least-squares program assuming Lorentzian line shapes.

## III. RESULTS AND COMPARATIVE STUDY

The space group of the hexagonal $CsFeCl_3$ and $RbFeCl_3$ is $D_{6h}^4$, with two molecules per unit cell. The Cs (or Rb) and Cl ions form a hexagonal closed-packed structure, and the $Fe^{2+}$ ions occupy the octahedral interstices, surrounded by six Cl ions (Fig. 1). Along the hexagonal $c$ axis, the $FeCl_6^{4-}$ octahedra make infinite chains.[2,3] The lattice parameters of $RbFeCl_3$ and $CsFeCl_3$ are given in Table I.

### A. Quadrupole splitting

Mössbauer measurements of $CsFeCl_3$ single crystals and powdered samples were done in the temperature range 4.2–300 °K. The Mössbauer spectrum shows a well-defined QS down to 1.4 °K. No sign of a phase transition was observed. At room temperature the splitting is 1.57 mm/sec. The intensity ratio between the $\pm\frac{3}{2} \rightarrow \pm\frac{1}{2}$ and $\pm\frac{1}{2} \rightarrow \pm\frac{1}{2}$ transitions was measured at room temperature at various angles[4] in order to determine the sign of the electric field gradient (EFG). These crystals possess a cleavage plane which contains the $c$ axis ($z$ axis of the EFG). For this purpose the angle $\theta$ is that between $\vec{k}_\gamma$ and the $c$ axis. For axial symmetry the sign of $V_{zz}$ is then determined. For our thin absorbers, we can use the expression[4]

$$\frac{I_{3/2\text{-}1/2}}{I_{1/2\text{-}\text{-}1/2}} = \frac{3(1-\cos^2\theta)}{5-3\cos^2\theta}$$

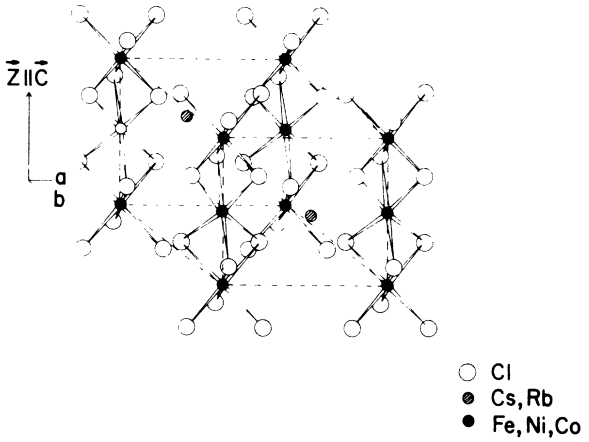


FIG. 1. Unit cell of $RbFeCl_3$ and $CsFeCl_3$.

for the ratio between the line intensities.

A typical spectrum of a powdered $CsFeCl_3$ absorber is shown in Fig. 2. The difference in the line intensities is apparently due to partial alignment, although an anisotropy in the $f$ factor could exist. The $Fe^{2+}$ ion in $CsFeCl_3$ is subjected, as in the $RbFeCl_3$ case, to the crystalline field produced by the surrounding $Cl^-$ octahedron. The weak-field approximation[5] can be applied here for the $^5D$ term of the single $Fe^{2+}$ ion. The $^5D(3d^6)$ state is then split by the cubic component of the crystalline field. There is a further splitting of the lowest ($^5T_{2g}$) levels by the spin-orbit interaction, $\lambda\vec{L}\cdot\vec{S}$, and by the residual trigonal component of the crystal field, $V_T = -\Delta(L_z^2 - 2)$, where $\Delta$ is the crystal field strength and the sign of $\Delta$ depends upon the nature of the distortion. Being interested in the trigonal distortion, we choose the quantization axis along [111]. The sign of $\Delta$ can be determined from the Mössbauer spectra of single crystals. It is seen from Fig. 3 that the ground state of the iron ion is a singlet for $\Delta<0$ and a doublet for $\Delta>0$. The sign of the $V_{zz}$ component of the EFG is then negative for the singlet; this is the case in $CsFeCl_3$, as well as in $RbFeCl_3$.[1] The total QS in a field of an axial symmetry, for the case where the nuclear relaxation time is long compared to the transition time between the $d$ orbitals, is given by

$$\Delta E_Q = \frac{e^2}{7}\langle r_{3d}^{-3}\rangle_{eff} Q \frac{\sum_i \langle i|(L_z^2-2)|i\rangle e^{-Ei/kT}}{\sum_i e^{-Ei/kT}} + \tfrac{1}{2}e^2 Q q_{latt}, \quad (1)$$

where $\langle r_{3d}^{-3}\rangle_{eff}$ includes both covalency and antishielding corrections. The last term is the lattice contribution to the QS,[6] including the Sternheimer antishielding factor,[7] and it can be significant. In an exact calculation assuming point charges,[8] the lattice contribution can be overestimated; for the case of the Fe-Cl bond, lattice summations have not been particularly successful, where the main problem lies in the assignment of effective charges to the ions. In the temperature region of 4.2 °K to room temperature, we have taken the lattice contribution as a (constant) free parameter. Fitting our QS data gives a lattice contribution of 0.08 ± 0.02 mm/sec for $CsFeCl_3$, as compared to 0.04 ± 0.01 mm/sec for $RbFeCl_3$. In the fitting procedure, the lattice contribution to the QS merely shifts the QS values but does not affect its temperature dependence. We also followed Ingalls's procedure[9] for estimating $q_{latt}$, namely,

$$q_{latt} \simeq -\frac{14(1-\gamma_\infty)\Delta}{e^2\langle r^2\rangle}, \quad (2)$$

and obtained similar results using a free $Fe^{2+}$, $\langle r^2\rangle_0 = 1.4$ a.u., and $(1-\gamma_\infty) = 12$.

TABLE I. Lattice parameters of $RbFeCl_3$ and $CsFeCl_3$.

| | $a$ (Å) | $c$ (Å) | Fe-Fe $c$ axis (Å) | Fe-Cl-Fe (deg) | Cl-Cl (Å) |
|---|---|---|---|---|---|
| $RbFeCl_3$ | 7.060 | 6.020 | 3.01 | 74.1 | 3.67 |
| $CsFeCl_3$ | 7.237 | 6.045 | 3.03 | 87.06 | 3.81 |

In order to understand the low-temperature behavior of the QS it is necessary to introduce an exchange interaction between the spins. We applied a treatment similar to that used in the case of $RbFeCl_3$,[1] where a Heisenberg interaction was assumed between the real spins of the $Fe^{2+}$ ions: $\mathcal{H} = -2J'_{ij}\vec{S}_i\cdot\vec{S}_j$. At low temperatures, we consider only the upper doublet and the singlet ground states, which are separated by $\sim 10$ cm$^{-1}$. Thus we can

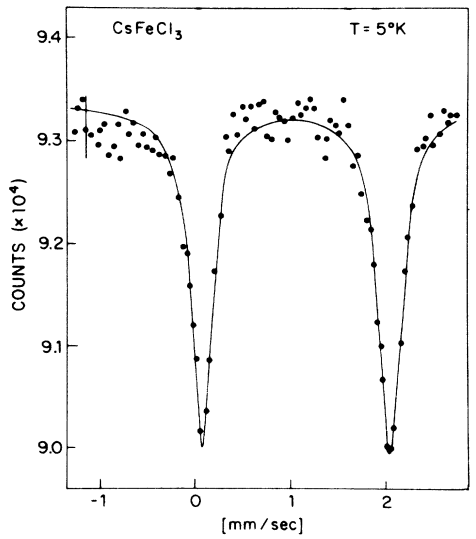


FIG. 2. Mössbauer spectrum of $CsFeCl_3$ powder at 5 °K.

use a fictitious spin $s = 1$ for the lowest three levels. In order to transform the real spin to an effective-spin system, we use conversion factors[10] $\alpha_{\parallel} S_z = S_z$; $\alpha_{\perp} S_x = S_x$; $\alpha_{\perp} S_y = S_y$. We then write the total Hamiltonian for the lowest $s = 1$ state of $Fe^{2+}$ interacting ions, assuming only nearest-neighbor interaction:

$$\mathcal{H} = D\sum_i S_i^{z2} - \sum_{\langle i,j\rangle}{}' [2J_{\parallel} S_i^z S_j^z + J_{\perp}(S_i^+ S_j^- + S_i^- S_j^+)], \qquad (3)$$

where $J_{\parallel} = \alpha_{\parallel}^2 J'$, $J_{\perp} = \alpha_{\perp}^2 J'$, $\alpha_{\parallel}^2/\alpha_{\perp}^2$ serves as a measure of the anisotropy.[10] $D$ is the single-ion anisotropy. As in $RbFeCl_3$,[1] we have solved this Hamiltonian, replacing (3) by a set of interacting $Fe^{2+}$ pairs. The results describe quite well the magnetic properties of the substance. A detailed calculation of the EFG including the magnetic interaction can be found in Ref. 1.

It is reasonable to assume an equal spin-orbit coupling[1] $\lambda$ in $CsFeCl_3$ and $RbFeCl_3$; $\lambda = 78 \pm 5$ cm$^{-1}$. $\langle r_{3d}^{-3}\rangle_{eff}$ is essentially the same in both substances. It is worth noting that this $\lambda$ is in good agreement with the covalency parameter $\alpha^2$ defined by Suchet and Bailly[11] for $FeCl_2$. The fit of the QS with these values versus temperature for $CsFeCl_3$ yields $-\Delta/\lambda \sim 0.85$ to $0.90$. For the low-temperature region ($S = 1$) the fit yields $D = 13$ cm$^{-1}$, $J_{\parallel} = 2.5 \pm 0.5$ cm$^{-1}$, $J_{\perp} = 5 \pm 1$ cm$^{-1}$. These values are consistent with the theoretical prediction $\alpha_{\perp}^2 J_{\parallel} = \alpha_{\parallel}^2 J_{\perp}$. The lattice contribution is 0.08 mm/sec and of opposite sign to that of the electronic contribution.

The experimentally observed QS as a function of $T$ for $CsFeCl_3$ is shown in Fig. 4(a). It can be compared with the calculation and QS of the $RbFeCl_3$ analyzed in Ref. 1 and shown here in Fig. 4(b). The contribution of the ground state ($s = 1$) was computed using the expression for $\langle L_z^2 - 2\rangle_T$ [cf. Eq. (B1) of Ref. 1]. The contribution of higher single-ion states was calculated without a magnetic interaction; the result is given by the solid lines in Figs. 4(a) and 4(b) (where $-\Delta/\lambda = 0.88$ and the lattice contribution is 0.08 mm/sec).

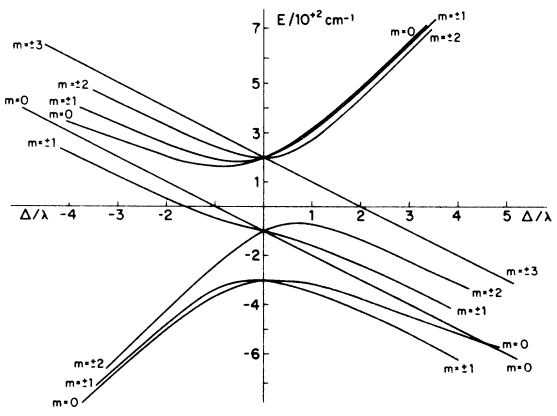


FIG. 3. $^5T_{2g}$ level diagram for axial field and spin-orbit interaction.

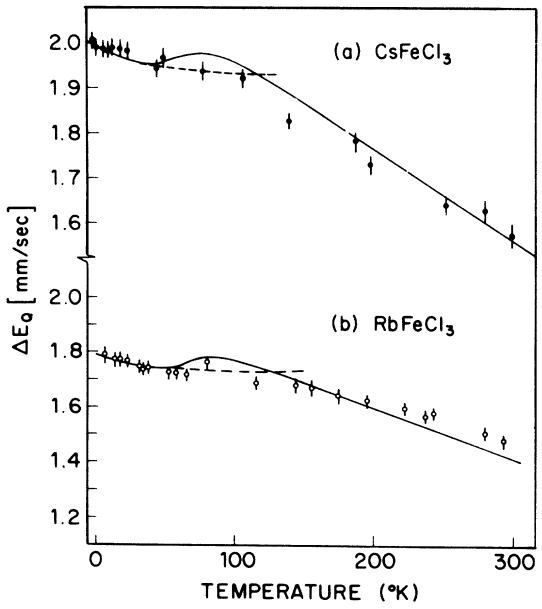


FIG. 4. Quadrupole splitting vs temperature: (a) $CsFeCl_3$; (b) $RbFeCl_3$. The dashed line is the contribution of the ground state ($s = 1$) using Eq. (3). The contribution of higher single-ion states is calculated without magnetic interaction. The total QS is represented by the solid line.

The results described above show that the magnetic interaction between iron ions along a chain is weaker in $CsFeCl_3$ than in the similar interaction in $RbFeCl_3$. This is consistent with our observation of no magnetic order in $CsFeCl_3$ down to 1.4°K, as compared to $RbFeCl_3$ (with a transition at 2.45°K). We also observed that in $CsFeCl_3$ the distance (Table I) between the $Fe^{2+}$ ions along the chain and the Fe-Cl distance are slightly larger compared to those in $RbFeCl_3$. Thus we expect a smaller magnetic interaction in $CsFeCl_3$. The QS in $CsFeCl_3$ is larger than that of $RbFeCl_3$; this is consistent with the existence of a larger crystal field in the former, as obtained from the QS data fit. The parameters obtained from the QS data for $RbFeCl_3$ and $CsFeCl_3$ are summarized in Table II.

TABLE II. Parameters for $CsFeCl_3$ and $RbFeCl_3$.

| | $\Delta/\lambda$ | $D$ (cm$^{-1}$) | $J_{\parallel}$ (cm$^{-1}$) | $J_{\perp}$ (cm$^{-1}$) |
|---|---|---|---|---|
| $RbFeCl_3$ | $(-0.75)-(-0.8)$ | $12 \pm 1$ | $5 \pm 1$ | $11 \pm 2$ |
| $CsFeCl_3$ | $(-0.85)-(-0.90)$ | $13 \pm 1$ | $2.5 \pm 1$ | $5 \pm 1$ |

### B. Dynamical parameters and isomer shifts

We compare the experimental and calculated results of $CsFeCl_3$ with those of $RbFeCl_3$: The center shift (CS) and the Debye-Waller factor $f$ depend on the lattice dynamics (phonon spectra) of the substances.[12]

The CS results from the second-order Doppler shift (SODS)[13] and from the isomer shift (IS):

$$\delta_{CS} = \delta_{IS} - \frac{E_0\langle v^2\rangle_T}{2c^2}. \tag{4}$$

In the harmonic approximation, the SODS is given by

$$\delta_{SODS} = \frac{\langle v^2\rangle_T}{2c^2} = \frac{1}{2c^2MN}\sum_\lambda\left[[e^{(Fe)}(\lambda)]^2\hbar\omega_\lambda \coth\left(\frac{\hbar\omega_\lambda}{2k_BT}\right)\right], \tag{5}$$

where $E_0 = 14.4$ eV, $M$ is the mass of the Mössbauer atom, $e^{(Fe)}(\lambda)$ is the part of the $\lambda$th-phonon polarization vector describing the motion of the $Fe^{2+}$ ion, $N$ is the number of Mössbauer ions, $k_B$ is the Boltzmann constant, and $c$ is the speed of light. The IS is given by

$$\delta_{IS} = \tfrac{1}{5}(2\pi z e^2)(R_{ex}^2 - R_{gr}^2)[|\psi_{abs}(0)|^2 - |\psi_{src}(0)|^2], \tag{6}$$

with the conventional notations.

The observed CS is the difference between source and absorber, and thus Eq. (4) expresses the experimental CS.

It can be seen that for the high-temperature limit, $k_BT \gg \hbar\omega_{mx}$, essentially optical vibrational modes or high-frequency parts of the phonon spectrum contribute to the SODS. In this limit we have

$$\delta_{SODS} \simeq \frac{3k_BT}{2Mc^2} + \frac{\hbar^2}{24k_BT}\sum_\lambda \frac{e^2(\lambda)}{N}\omega_\lambda^2 + \cdots .$$

We can therefore use the Einstein model to calculate the SODS.

The temperature dependence of the CS as seen from our results is therefore attributed to the SODS. This is equivalent to the assumption that the $s$-electron density is temperature independent in the temperature range of our experiment. We can then apply the following expression to fit the expected behavior of the experimental results[14]:

$$\delta_{CS}\ (\text{mm/sec}) = \delta_0 - 7.306\times10^{-4}\Theta_E\left(\frac{1}{e^{\Theta_E/T}-1} + \frac{1}{2}\right), \tag{7}$$

where $\delta_0$ includes the constant SODS of the source.

The experimental CS $T$ dependence is shown in Fig. 5. The shift is relative to the centroid of a standard $Na_2Fe(CN)_5(NO)\cdot 2H_2O$ absorber:

$RbFeCl_3$: $\delta_0 = 1.583$ mm/sec,
$\Theta_E = (310 \pm 45)^\circ$K,

$CsFeCl_3$: $\delta_0 = 1.577$ mm/sec,
$\Theta_E = (204 \pm 22)^\circ$K.

The isomer shifts of the Rb and Cs compounds are essentially the same. This is expected, since the $Fe^{2+}$ has identical nearest neighbors in the two compounds. Thus the *center*-shift difference in the two crystals is apparently due to differences in the vibrational spectrum projected on the $Fe^{2+}$ ions in the crystal (Fig. 6).

We use the calibration of the isomer shift for the total $s$-electron density as a function of $x$ in the $3d^6 4s^x$ configuration,[15] with respect to nitroprusside standard: A contribution of 10–20% of the 4$s$ electron is expected. If this is related to the degree of covalency and expressed by $\alpha^2(\lambda = \alpha^2 \times \lambda_{\text{free ion}})$, we find consistency with that obtained previously. If we take $\langle r_{3d}^{-3}\rangle \cong \alpha^2\langle r^{-3}\rangle_0$, $\langle r^{-3}\rangle_0 \cong 5.1a_0^{-3}$, then $Q = 0.24$ b. (In this case,[16] $\langle r^{-3}\rangle_{\text{eff}} \cong 3.2a_0^{-3}$, which is close to the 0.21 b obtained elsewhere.[17,18])

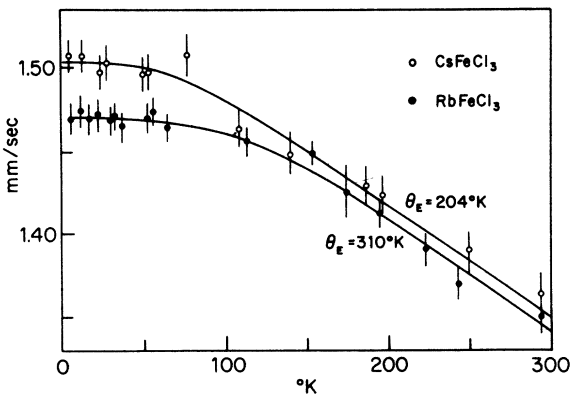


FIG. 5. Experimental CS vs $T$. The shifts are given relative to the centroid of a standard $Na_2Fe(CN)_5(NO)\cdot 2H_2O$.

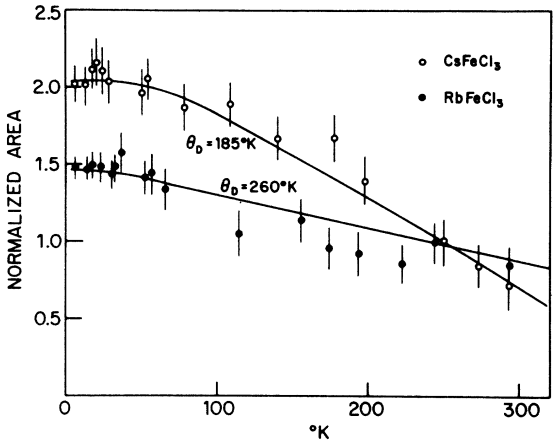


FIG. 6. Normalized Mössbauer spectral area vs $T$.

[1]P. A. Montano, E. Cohen, H. Shechter, and J. Makovsky, Phys. Rev. B 7, 1180 (1973).
[2]H. J. Seifert, Z. Anorg. Allgem. Chem. 342, 1 (1966).
[3]G. R. Davidson, M. Eibschutz, D. E. Cox, and V. J. Minkiewicz, in *Proceedings of the Seventeenth Conference on Magnetism and Magnetism and Magnetic Materials, Chicago*, 1971, edited by C. D. Graham and J. J. Rhyne (AIP, New York, 1972).
[4]P. Zory, Phys. Rev. 140, A140 (1965).
[5]J. S. Griffith, *The Theory of Transition Metal Ions* (Cambridge U. P., London, 1961).
[6]B. Bleaney and K. W. H. Stevens, Rept. Prog. Phys. 16, 108 (1953).
[7]R. M. Sternheimer, Phys. Rev. 84, 244 (1951).
[8]A. J. Novik and M. Kaplan, Phys. Rev. 159, 273 (1967).
[9]R. Ingalls, Phys. Rev. 133, A787 (1964).
[10]M. E. Lines, Phys. Rev. 131, 546 (1963).
[11]J. P Suchet and F. Bailly, Ann. Chem. Phys. 10, 517 (1965).
[12]R. Ingalls, Phys. Rev. 188, 1045 (1969).
[13]B. D. Josephson, Phys. Rev. Lett. 4, 341 (1960); R. V. Pound and E. A. Rebka, Phys. Rev. Lett. 4, 274 (1960).
[14]D. P. Johnson and R. Ingalls, Phys. Rev. B 1, 1013 (1970).
[15]L. R. Walker, E. K. Wertheim, and V. Jaccarino, Phys. Rev. Lett. 6, 98 (1961); J. J. Spijkerman, F. C. Ruegg, and Leopold May, in *Mössbauer Effect Methodology*, edited by I. J. Gruverman (Plenum, New York, 1966), Vol. 2, p. 85.
[16]A. Abragam and F. Bourton, Compt. Rend. 252, 2404 (1961); R. E. Watson and A. Freeman, Phys. Rev. 123, 2027 (1961).
[17]V. I. Goldanskii and R. H. Herber, *Chemical Applications of Mössbauer Spectroscopy* (Academic, New York, 1968).
[18]R. M. Housley and F. Hess, Phys. Rev. 146, 517 (1966).